Mon. Not. R. Astron. Soc. **000**, 000–000 (0000) Printed 29 April 2014 (MN LATEX style file v2.2)

Analysis of bulk void regions

Sebastian Bustamante ⋆[1] Jaime E. Forero-Romero[2]

[1]*Instituto de Física - FCEN, Universidad de Antioquia, Calle 67 No. 53-108, Medellín, Colombia*
[2]*Departamento de Física, Universidad de los Andes, Cra. 1 No. 18A-10, Edificio Ip, Bogotá, Colombia*

29 April 2014

ABSTRACT

Key words: Cosmology: large-scale Structure of Universe, galaxies: star formation - line: formation

1 INTRODUCTION

The spatial distribution of galaxies describes a web-like pattern, the so-called cosmic web. Today it is understood that such configuration is driven by gravitational instabilities. ...

Relevant information about previous works and current state of the art.

2 THE SIMULATION

As it was previously mentioned, we use an unconstrained cosmological simulation, the Bolshoi simulation, to identify the possible large scale environment of the Local Group. This is a similar approach to the one already used by **[reference here]**.

The Bolshoi simulation follows the non-linear evolution of a dark matter density field on a cubic volume of size $250h^{-1}$Mpc sampled with 2048^3 particles. The cosmological parameters in the simulation are $\Omega_{\rm m} = 0.27$, $\Omega_\Lambda = 0.73$, $h = 0.70$, $n = 0.95$ and $\sigma_8 = 0.82$ for the matter density, cosmological constant, dimensionless Hubble parameter, spectral index of primordial density perturbations and normalization for the power spectrum. The mass of each particle in the simulation is $m_{\rm p} = 1.4 \times 10^8 h^{-1}{\rm M}_\odot$. We identify halos with two algorithms, the Friends-of-Friends **[reference here]** algorithm and the Bound Density Maximum algorithm.

3 ALGORITHMS TO QUANTIFY THE COSMIC WEB

3.1 The tidal web (T-web)

The first algorithm we use to identify the cosmic web is based upon the diagonalization of the tidal tensor, defined as the Hessian of a normalized gravitational potential

$$T_{\alpha\beta} = \frac{\partial^2 \phi}{\partial x_\alpha \partial x_\beta} \tag{1}$$

where the physical gravitational potential has been rescaled by a factor $4\pi G\bar{\rho}$ in such a way that ϕ satisfies the following equation

$$\nabla^2 \phi = \delta, \tag{2}$$

where $\bar{\rho}$ is the average density in the Universe, G is the gravitational constant and δ is the dimensionless matter overdensity.

3.2 The velocity web (V-web)

We also use a kinematical method to define the cosmic-web environment in the simulation. The method has been thoroughly described in XXX and applied to study the shape and spin alignment in the Bolshoi simulation here XX. We refer the reader to these papers to find a detailed description of the algorithm, its limitations and capabilities. Here we summarize the most relevant points for the discussion.

The V-web method for environment finding is based on the local shear tensor calculated from the smoothed DM velocity field in the simulation. The central quantity is the following dimensionless quantity

$$\Sigma_{\alpha\beta} = -\frac{1}{2H_0}\left(\frac{\partial v_\alpha}{\partial x_\beta} + \frac{\partial v_\beta}{\partial x_\alpha}\right) \tag{3}$$

where v_α and x_α represent the α component of the comoving velocity and position, respectively. $\Sigma_{\alpha\beta}$ can be represented by a 3×3 symmetric matrix with real values, that ensures that is possible to diagonalize and obtain three real eigenvalues $\lambda_1 > \lambda_2 > \lambda_3$ whose sum (the trace of $\Sigma_{\alpha\beta}$) is proportional to the divergence of the local velocity field smoothed on the physical scale $\mathcal{R}$.

The relative strength of the three eigenvalues with respect to a threshold value λ_{th} allows for the local classifica-

⋆ sbustama@pegasus.udea.edu.co

tion of the matter distribution into four web types: voids, sheets, filaments and peaks, which correspond to regions with 3, 2, 1 or 0 eigenvalues with values larger than λ_{th}. Below we shall discuss a novel approach to define an adequate threshold value based on the visual impression of void regions, furthermore we study other possible values based on other visual features of the cosmic web.

3.3 The cosmic web in Bolshoi

Both established schemes to quantify the cosmic web depend on continuous and smooth physical quantities, i.e the peculiar velocity field and the density field. To calculate these quantities, a discretization over the volume of the simulation is performed, so all the properties are reduced to single values associated to discrete cells. According to this, we divide the overall volume into $(256)^3$ cells, so each cell has an associated comoving cubic volume of 0.98 Mpc h^{-1}. Finally, in order to reduce possible effects due to the discretization process, a gaussian softening is performed between neighbour cells.

Once defined the numerical details about both classification schemes, we shall analyse the dependence on the threshold value λ_{th} for each one. For this, we shall use the distribution of dark matter halos as tracer of the underlying matter field in order to be more consistent with available observational data. First, we analyse distributions of mass and peculiar velocity in order to assign typical values to each type of environment. In the figure 1 we calculate both distributions for web schemes and using the FOF catalogue of the simulation. Thick lines correspond to the median of the distribution and filled regions limited by dashed lines correspond to quartiles Q_1 and Q_3, it means, 50% of all halos are within such regions for every λ_{th} value and for each type of environment. We rather use median and quartiles as measure of dispersion because there are some very unusual and extreme values that makes the usual analysis based upon means and standard deviations less reliable.

A first interesting feature of the figure 1 is the median mass for each region. In the case of the T-web, although dispersions of the distribution of mass for each environment are considerably overlapped each other, the median value is very well-differentiated among types of environment, indicating that it is possible to assign typical values of mass to each region, and being consistent with expectations, where low mass halos are typical in voids until high mass halos in knots. For the case of the V-web scheme, all medians and dispersions are completely overlapped, specially for values grater than the optimal λ_{th} value, indicating that it is not possible to assign typical mass ranges to each environment as quantified by this scheme. For peculiar velocities, this situation is opposite, where V-web scheme is much more adequate to assign typical distributions of velocity to each environment. Although T-web also makes a differentiation in the distributions of velocity, this is very slight compared with the V-web case. These results can be explained by appealing the physical origin of each web scheme. As T-web is based upon the Hessian matrix of the potential field, it is expected all quantities related to the potential, like density field and distribution of halos mass, are well-differentiated among each region, while for the V-web scheme, based upon the shear velocity tensor, all dynamical quantities, as the peculiar velocity field and the distribution of halos velocity are alike expected to be well-differentiated among regions as quantified by this scheme.

Finally, we also calculate typical distributions of the density and peculiar velocity fields on the volume cells associated to each type of environment, obtaining completely analogous results. Furthermore, we use a BDM catalogue of the simulation as well, obtaining very similar conclusions.

4 FINDING BULK VOIDS

According to the recent growing interest in studying galaxy formation in low-density regions as cosmological tests, classifying void regions is becoming an important task in cosmology. Most of those classification schemes for voids in cosmological simulations are based upon the density field, setting a cut off value below which some region becomes a void **[references]**. Some more advanced classification schemes are based on Voronoi tessellations applied over the tracer particles of the simulation in order to compute the density field. Then, through a watershed transform, a hierarchy of void regions are found **[references, ZOBOV algorithm]**.

As has been established **[references]**, both schemes presented in the previous section (V-web and T-web) for classifying the cosmic web present many advantages compared with classification schemes based completely upon the density field, e.g. a more robust description of the dynamic a kinematic of the cosmic web, a more reliable quantification of the visual impression, among others. With the aim of exploiting all of these advantages, we propose here a novel approach to classify voids in cosmological simulations based entirely on the web schemes.

The original version of the T-web scheme **[reference, Hahn]** was not successful at reproducing the visual impression of the cosmic web, however, with the introduction of a threshold parameter **[reference, Forero-Romero]**, this scheme, and even the V-web **[reference, Hoffman]**, improved enormously. As this free parameter controls the visual impression provided by each scheme, phenomenons like percolation depends on it as well. Percolation is one of the key features of the structure of void regions, indicating how voids are merged among them, and how they permeate all the cosmic web.

In order to overcome the percolation of voids in our classification scheme, we introduce the fractional anisotropy as defined in **[reference, Libeskind]**.

$$FA = \frac{1}{\sqrt{3}}\sqrt{\frac{(\lambda_1-\lambda_3)^2+(\lambda_2-\lambda_3)^2+(\lambda_1-\lambda_2)^2}{\lambda_1^2+\lambda_2^2+\lambda_3^2}} \tag{4}$$

where the eigenvalues are taken from any of the two web schemes. This index, such as it is defined, allows quantifying the local anisotropy degree of the cosmological environment, where $FA = 0$ corresponds to highly isotropic regions and $FA = 1$ anisotropic ones.

In the figure 2 we calculate the FA field over the simulation for both web schemes. The first interesting feature of this figure is the degeneration presented for knots and central regions of voids, where both of them exhibit low to middle values of the FA, indicating a high isotropy regarding the physical property quantified by each web scheme, i.e. the density field for the T-web and the peculiar velocity for the V-web. For the T-web, the FA field around knots presents a very narrow distribution, whereas for the V-web the same distribution is more spread. This can be explained appealing to the low dispersion of the density field with respect to the peculiar velocity in highly non-linear regions like knots. For more linear regions like voids, the behaviour of the FA field is quite similar between both schemes, what is consistent with the equivalence of the T-web and the V-web in the linear regime **[reference, Hoffman]**.

According to the classification scheme adopted for the cosmological environment, voids are regions where $\lambda_3 \leqslant \lambda_2 \leqslant \lambda_1 \leqslant \lambda_{th}$, this implies that the boundaries of void regions are controlled completely by the λ_1 eigenvalue of the web scheme and the threshold value. Therefore, as we increase the threshold value $\lambda_t h$, all voids grow up progressively through contours of λ_3 field until certain critical value where voids are very large so the visual impression is no longer reliable.

5 PROPERTIES OF VOIDS

Once defined the proper scheme to classify bulk voids in the simulation, we proceed to analyse their physical properties, like the inertia values, the density and peculiar velocities profiles as calculated over the grid and profiles of number of halos.

5.1 Shape of voids

Quantifying the shape of voids is gaining importance due to cosmological tests such as the Alcock-Paczynski test **[Sutter, et.al (2012)]**, so we compute here the reduced inertia tensor through the next expression in order to determine shape distributions of bulk voids.

$$\tau_{ij} = \sum_{l} \frac{x_{l,i} x_{l,j}}{R_l^2} \tag{5}$$

where l is an index associated to each cell of the current region, i and j indexes run over each spatial direction and finally R_l is defined as $R_l^2 = x_{l,1}^2 + x_{l,2}^2 + x_{l,3}^2$. All positions are measured from the respective geometric center of each void.

The eigenvalues of the reduced inertia tensor, i.e. the principal moments of inertia, are used to quantify the shape of each bulk void. They are denoted as τ_1, τ_2 and τ_3 such that $\tau_1 \leqslant \tau_2 \leqslant \tau_3$. In Figure **??** we show the computed distributions for τ_1/τ_2 and τ_2/τ_3 for voids larger than 8 cells in order to avoid statistic fluctuations due to small regions. We rather calculate histograms for these ratio quantities instead of each single value in order to avoid using an arbitrary normalization. For both schemes, it can be noticed that the shape distribution is completely spread out, thereby indicating a non-preferred geometry of void regions, which is in agreement with the well established high anisotropy of matter flows associated to this type of region.

For a better quantification, we also perform a classification of the shape of voids by setting a threshold in the analysed ratio quantities. An anisotropic or tri-axial shape correspond to voids where $\tau_1/\tau_2 < 0.7$ and $\tau_2/\tau_3 < 0.7$, where there is not any symmetry among the principal directions. We find about 57.2% $\sim$ 61.0% of total voids consistent with this shape, for the T-web and V-web respectively. A pancake or quasi-oblate shape is associated to voids where $\tau_1/\tau_2 < 0.7$ and $\tau_2/\tau_3 > 0.7$. We found 13.1% $\sim$ 17.9% of consistent voids. Filamentary or quasi-prolate voids satisfy $\tau_1/\tau_2 > 0.7$ and $\tau_2/\tau_3 < 0.7$, with 25.4% $\sim$ 18.1% of all voids. Finally, isotropic or quasi-spheric voids are found when $\tau_1/\tau_2 > 0.7$ and $\tau_2/\tau_3 > 0.7$, with 4.2% $\sim$ 3.1% of total voids compatible with this shape. The threshold value of 0.7 adopted here for the ratios of the moments of inertia is just for illustrative purposes, where such distinction is rather fuzzy and continuous. However, the previous analysis allows us to conclude that voids are quite asymmetric structures.

5.2 Density profile of voids

Describing the density profiles of voids is quite important in order to compare and match simulation with observational surveys, allowing possible constrains for different cosmology models **[Hamaous, et.al 2014]**. Here, and taking into account the previous results, we rather use an ellipsoidal approximation to describe and fit the shape of bulk voids, so we use the next ellipsoidal radial coordinate to describe density profiles.

$$r^2 = \frac{x^2}{\tau_1^2} + \frac{y^2}{\tau_2^2} + \frac{z^2}{\tau_3^2}, \qquad 0 \leqslant r \leqslant 1 \tag{6}$$

where we take the principal moments of inertia $\{\tau_i\}$ as the lengths of the principal axes of the ellipsoid and each one of the cartesian coordinates as measured in the rotated frame of each void.

We use the same analytic density profile that **[Hamaous, et.al 2014]** to fit the numerical density profiles of our voids.

$$\delta_v(r) = \delta_c \frac{1 - (r/r_s)^\alpha}{1 + (r/r_v)^\beta} \tag{7}$$

6 CONCLUSIONS

ACKNOWLEDGMENTS

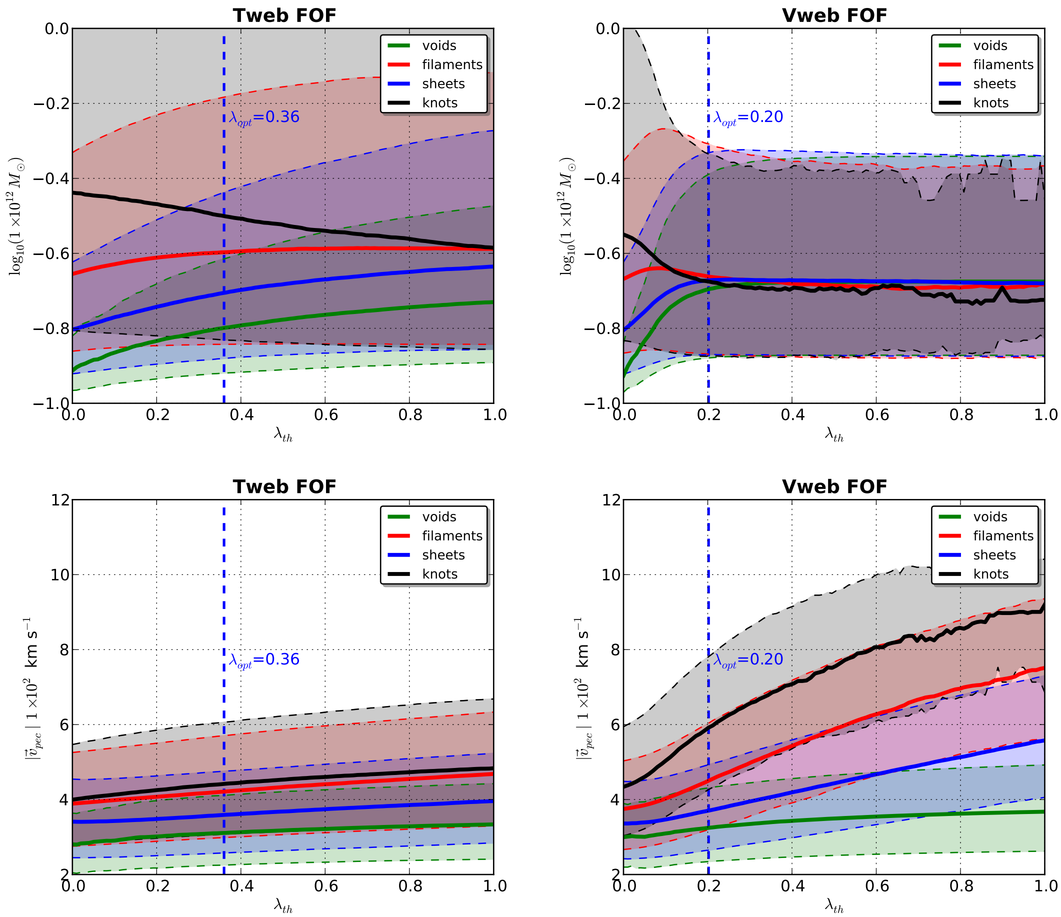

Figure 1. Distribution of masses of dark matter halos according the region where they are embedded for both web schemes (upper panels) and of peculiar velocity (lower panels). It can be noticed that the T-web scheme selects different mass ranges according to the environment, while the V-web scheme is better selecting ranges of peculiar velocity of the dark matter halos. This can be understood taking into account the physical origin of each web scheme.

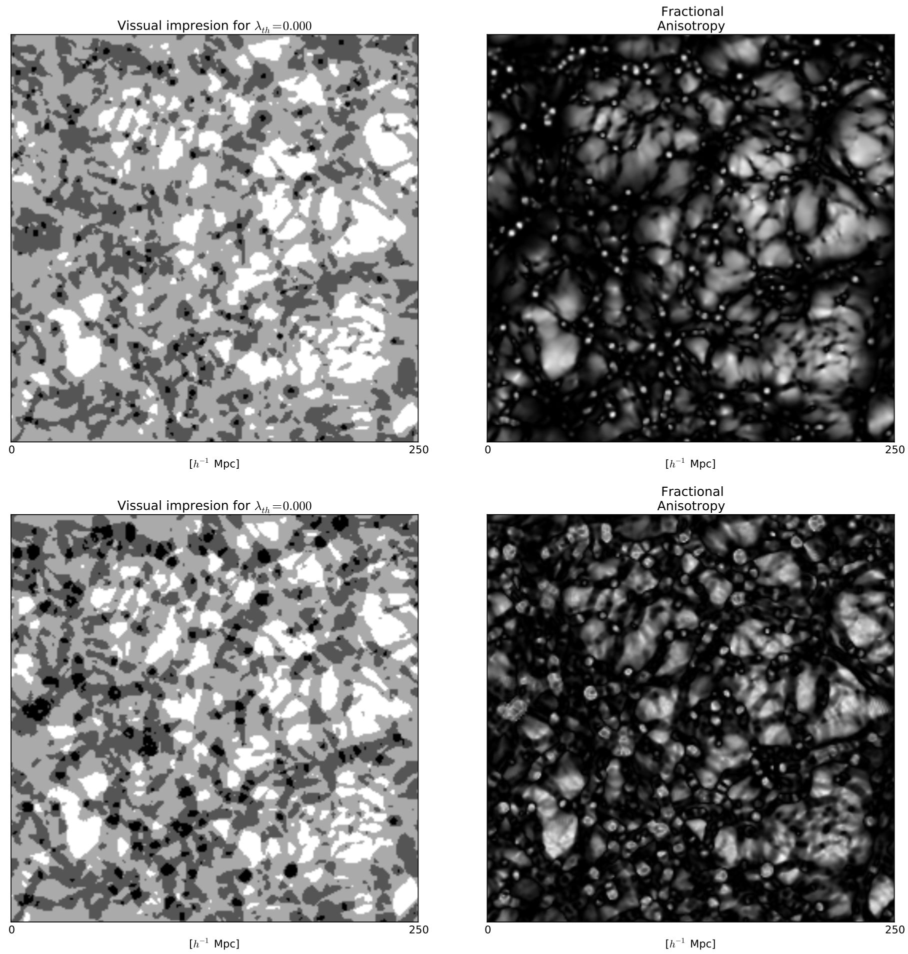

Figure 2. In left panels is shown the visual impression of the cosmic web for each web scheme (T-web, upper panels. V-web, lower panels) obtained for $\lambda_{th} = 0.0$. It can be seen each one of the defined type of environments, where voids corresponds to white zones, sheets to gray, filaments to dark gray and finally knots to black regions. In the right panels is shown the fractional anisotropy field for the same slide of the simulation and for each web schemes, where black regions correspond to FA= 1 and white regions to FA= 0. It can be noticed the degeneration of low values of FA for knots and central regions of voids, while high values of FA (FA $\lesssim 1$) are consistent with filaments and highly planar sheets.